Journal of Applied Geophysics 134 (2016) 226–234

Contents lists available at ScienceDirect

Journal of Applied Geophysics

journal homepage: www.elsevier.com/locate/jappgeo

Water prospection in volcanic islands by Time Domain Electromagnetic (TDEM) surveying: The case study of the islands of Fogo and Santo Antão in Cape Verde

F.J. Martínez-Moreno *, F.A. Monteiro-Santos, J. Madeira, I. Bernardo, A. Soares, M. Esteves, F. Adão

Instituto Dom Luiz, Universidade de Lisboa, Faculdade de Ciências, Campo Grande, Edif. C8, Lisboa, Portugal

ARTICLE INFO

Article history:
Received 13 May 2016
Received in revised form 22 August 2016
Accepted 15 September 2016
Available online 19 September 2016

Keywords:
Time Domain Electromagnetics (TDEM)
Cape Verde
Volcanic islands
Groundwater resources
Trade winds

ABSTRACT

Water demand in islands, focused in agriculture, domestic use and tourism, is usually supplied by groundwater. Thus the information about groundwater distribution is an important issue in islands water resources management. Time Domain Electromagnetic (TDEM) provides underground resistivity distribution at greater depths and is of easier application than other methods. In this study TDEM technique was used for groundwater prospection in two volcanic islands with water supply problems, the islands of Fogo and Santo Antão in the Republic of Cape Verde. The 10 islands of Cape Verde Archipelago, located off the coast of Senegal (W Africa), present a semi-arid climate and thus suffer from irregular and scarce precipitation. In the Island of Fogo 26 TDEM soundings, presenting an area distribution, were performed on the SW flank of the volcanic edifice. These allowed obtaining a 3D model composed of 5 layers parallel to the topographic surface separated by 50 m depth down to −250 m. The results indicate the presence of the water-table at a depth of 150 m in the lower ranges of the W flank of the island, and at >200 m depth in the area above 250 m above sea level (a.s.l.). In the Island of Santo Antão 32 TDEM soundings, distributed along 5 linear profiles, were obtained on the north-eastern half of the island. The profiles are located in two regions exposed to different humidity conditions to the N and S of the main water divide. The northern flank receives the dominant trade winds first and most of the precipitation and, therefore, the water-table is shallower (~50 m depth) than in the S (~100 m depth). Our study demonstrates the applicability and usefulness of the TDEM method for groundwater prospection in high resistivity contexts such as in volcanic islands.

1. Introduction

Volcanic ocean islands represent isolated hydrogeological systems. The hydrogeological characteristics of each island are dependent on climate conditions (that determine precipitation regimes, vegetation cover and soil development), topography, geology (including lithology, structure and rock permeability), land use and water resources exploitation (Healy, 2010). The most relevant geological structures present in volcanic islands from a hydrogeological standpoint are: (i) the presence of an island basement usually presenting low permeability; (ii) the geometry of dike swarms that control the aquifers behaviour; (iii) the occurrence of impermeable layers (i.e. paleosols, sediments or compacted ash deposits) interbedded in the lava sequences supporting perched aquifers; and (iv) weathered landslide breccias at the base of large flank collapse surfaces acting as impermeable layers (Martí et al., 1997; Santamarta Cerezal, 2013; Marques et al., 2014).

Aquifer recharge in islands may occur in two different ways: by direct rainfall and by fog precipitation. The direct rainfall is conditioned by the island geographical location, altitude and morphology. The second type of aquifer recharge in islands is produced by condensation of clouds, formed by adiabatic cooling of trade winds forced upwards, which may represent 1.5 to 3 times the amount of rainfall (Santamarta Cerezal and Seijas Bayón, 2010; Figueira et al., 2013). This kind of winds transports a high amount of water that is captured by the forest or is directly discharged when it founds topographic barriers (Johnson et al., 2014).

In volcanic islands, the proportion between runoff, evapotranspiration and groundwater recharge is determined by surface permeability, soil water storage, topographic slope, bare-soil evaporation and plant transpiration (Flint et al., 2013). Usually, volcanic islands do not have runoff water in the form of permanent rivers. This is due to incipient soil development at high elevations in addition to significant fracturing of rock outcrops, which favours water infiltration. Thus, most infiltration and groundwater recharge occurs in the higher reaches of the islands resulting from the combination of higher precipitation, greater permeability induced by fractures, and the frequent occurrence of closed basins (craters, calderas, and other closed depressions of various types) (Heilweil et al., 2009).

Dike intrusions are a distinctive feature in volcanic islands hydrogeology because they act as water flow barriers within the geologic structure

* Corresponding author.
E-mail address: fjmoreno@fc.ul.pt (F.J. Martínez-Moreno).

http://dx.doi.org/10.1016/j.jappgeo.2016.09.020
0926-9851/

generating isolated aquifers at different water-table altitudes. These volcanic structures typically present near-vertical dips and thicknesses less than 3 m. Dikes behave as impermeable walls that divide the island underground into separated compartments from a hydrogeological point of view (MacDonald et al., 1983). Each of them represents local aquifers ranging from low altitude – low gradient regional water-tables located near sea level (areas usually characterized by low topographic slope), to high altitude – high gradient water-tables in topographically higher regions (usually more rugged morphologies) (Liu et al., 1983; Jackson and Lenat, 1989; Gingerich and Oki, 2000).

Water demand in islands is mostly due to agriculture activity and to domestic use. Water consumption by touristic demand, which requires increased amounts of water, may also play a significant role depending on the archipelago (López-Guzmán et al., 2015). In the islands most of the water used in human activities is groundwater since surface water is commonly scarce or even absent (Custodio, 1978). For this reason, the information on groundwater distribution is an important issue in island water resources management. In areas where wells, boreholes and drills are abundant, hydrogeological studies can be performed directly. In the absence of wells or when the spacing between them is large, the hydrogeological information they may provide is insufficient and non-representative. In this context, the search for groundwater resources must be addressed by geophysical prospection.

Time Domain Electromagnetic (TDEM) – or *transient* – is a reliable geophysical technique to determine groundwater distribution in a specific area. TDEM method provides underground resistivity distribution so that the presence of the fresh water-table or saltwater produces a sudden change in resistivity from high resistivity values (in unsaturated rocks) to low or very low ones (in saturated rocks). This technique has been employed in various specific geological contexts for groundwater prospection (Goldman et al., 1994; Sananikone, 1998; Descloitres et al., 2000; Yechieli et al., 2001; Hoareau et al., 2007; Descloitres et al., 2013; Ruiz-Constán et al., 2015).

This study was primarily motivated by the need to obtain information about groundwater distribution in areas with water supply problems in the islands of Fogo and Santo Antão in the Cape Verde archipelago (Central Atlantic Ocean). Thus, the aim of this work is mainly focused in determining groundwater distribution using TDEM data in these two islands. With this purpose a network of TDEM station was installed in areas with no previous geophysical data.

2. Geological framework

The ten major islands forming the Cape Verde Archipelago (República de Cabo Verde, Fig. 1a) display a horseshoe shape open to the west. The archipelago is located 600 km to the W of the coast of Senegal (W Africa). The islands are traditionally divided into two groups related to the dominant Trade Winds: the Barlavento (windward) Group comprising the islands of Santo Antão, São Vicente, Santa Luzia, São Nicolau, Sal, and Boavista, and the Sotavento (leeward) Group that includes the islands of Brava, Fogo, Santiago and Maio. The archipelago was built on Late Jurassic to Cretaceous oceanic crust on top of a major topographic anomaly — the Cape Verde Rise. The magmatism is considered to be the result of a mantle plume (White, 1989) and the ages of the oldest subaerial lavas suggest that the islands emerged during the Miocene (Mitchell et al., 1983; Torres et al., 2002; Plesner et al., 2003; Duprat et al., 2007; Holm et al., 2008; Madeira et al., 2010; Dyhr and Holm, 2010; Ramalho et al., 2010; Ancochea et al., 2010; Ancochea

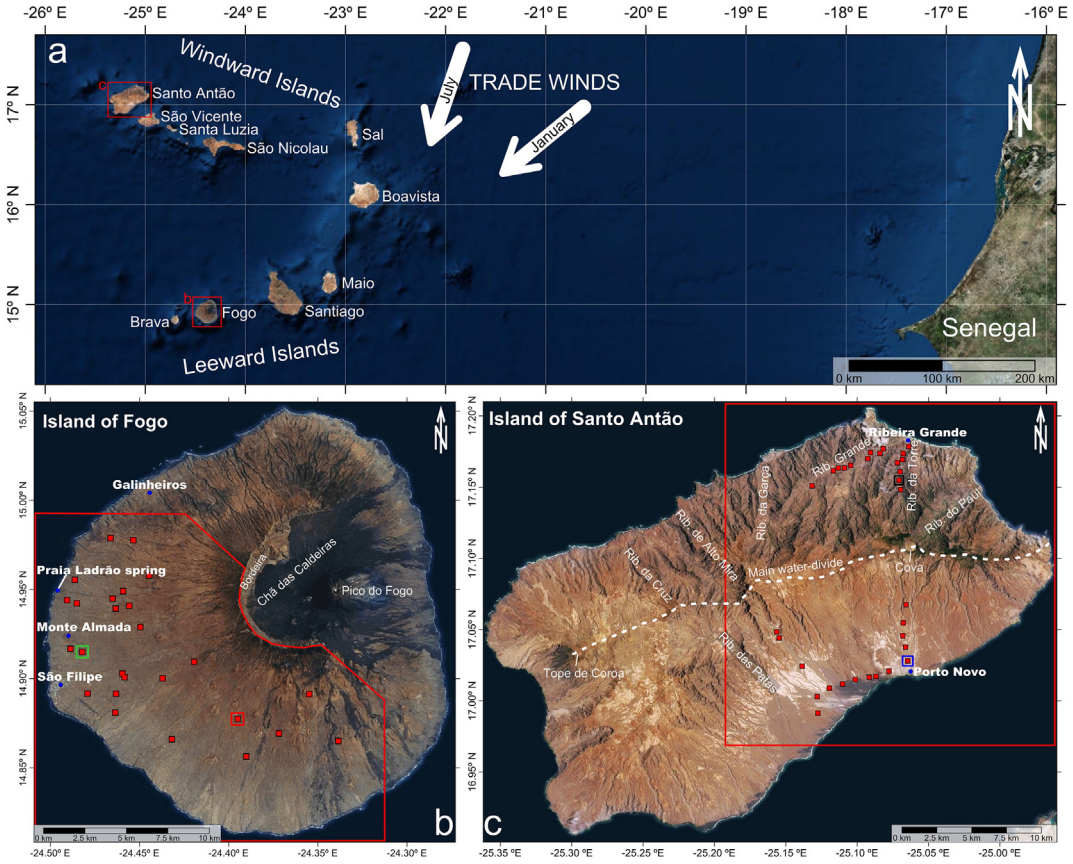

Fig. 1. Geographical location of the Cape Verde archipelago and the studied islands (a). The location of TDEM soundings (red squares) is shown on orthophoto images of the study areas of Fogo (a) and Santo Antão (b). The study area of each island is indicated by a red line. The red, green, blue and brown squares identify the TDEM stations displayed in Fig. 3. (For interpretation of the references to colour in this figure legend, the reader is referred to the web version of this article.)

et al., 2014; Ancochea et al., 2015). The morphology of the islands is related to their age, with the younger islands presenting vigorous morphologies that contrast with the razed topography of easternmost older islands of Sal, Boavista and Maio.

The islands of Santo Antão and Fogo, two of the youngest, are located on the western tips of the two arms of the U-shaped archipelago. Fogo is the fourth largest island with a surface area of 476 km^2, culminating at 2829 m above sea level (a.s.l.) at Pico do Fogo which represents the highest elevation in the archipelago. The island is formed by a major conical and slightly asymmetrical Quaternary strato-volcano. It is mostly formed by basanitic lava flow piles with minor intercalations of pyroclastic and sedimentary layers (Fig. 2a). A small outcrop of an older (Pliocene) basement formed by intrusive carbonatites (Hoernle et al., 2002) covered by lavas from the Intermediate and Younger volcanic units lies 3 km to the N of the city of São Filipe. The summit of the volcano is truncated by an 8 km-wide depression (Chã das Caldeiras; Fig. 1b) open to the E and surrounded on the other sides by an almost vertical wall (Bordeira). Rising from the flat floor of the depression is the young cone of Pico do Fogo. The depression is interpreted as the result of a major collapse of the E flank of the volcanic edifice (Day et al., 1999) or a combination of two caldera collapses followed by the failure of the E flank (Brum da Silveira et al., 1997; Madeira et al., 2008; Ramalho et al., 2015). The outer slopes are covered by pre-historical post-collapse lava flows issued from parasitic cones, aligned on radial and concentric feeder dikes, extending from the caldera rim to sea level. The NE flank is displaced by a graben structure bound by NE-SW fault scarps, the most conspicuous of which is the Galinheiros Fault. The caldera and the flank collapse scar are floored by historical lava flows and locally by lahars (Ribeiro, 1960; Torres et al., 1998). The latest Fogo eruption occurred on November 23rd, 2014 and lasted until early February 2015.

The island presents a constructive volcanic morphology that is perturbed by the caldera and flank collapse depressions. The drainage pattern is radial in the outer flanks of the main volcano. Inside the depression there is no developed drainage except for the E flank of Pico do Fogo where several streams are incised on the pyroclasts and lahar deposits. The morphological asymmetry is, like in Santo Antão, the result of the dominant north-easterly trade winds. Most precipitation falls on the windward flank and thus the slopes are steeper and the streams more incised. The N littoral is also characterized by taller sea cliffs.

Santo Antão is the second largest island in Cape Verde with a surface area of 779 km^2 and rising to 1980 m a.s.l. at Tope de Coroa volcano, the second highest elevation in the archipelago. Geologically the island corresponds to an elongated NE-SW trending shield volcano that was fed by fissure volcanism along a dense dike swarm (Fig. 2b). The dike swarm follows the axial regions of the island and is well exposed in the deepest valleys of Ribeira das Patas, Ribeira da Garça and Ribeira Grande (Fig. 1c). The orientation of the later valley is certainly controlled by the dike structure since it is perpendicular to the slope of the N flank. The dominant direction of the dikes is NE-SW and its density decreases towards the coastal areas. These dikes fed the different building phases of the volcanic edifice. The most voluminous volcanism, corresponding to the main shield building phase (Older and Intermediate Volcanics, Holm et al., 2006), is represented by a thick pile of dominantly basanitic lava flows; in the northeast tip the sequence culminates with pyroclastic flow deposits related to hydromagmatic eruptions to the S and northeast of Cova crater. This volcanic building was later covered by smaller volume volcanic phases (Younger Volcanics, Holm et al., 2006). Besides basanitic lava flows, the younger volcanic phases produced abundant explosive deposits of more evolved compositions (phonolite) represented by plinian pumice fall, ignimbrite and block and ash flow deposits (Eisele et al., 2015).

The morphology of Santo Antão reflects its volcanic structure and is mostly a constructive surface corresponding to a narrow plateau punctuated by monogenetic cones and craters that descends towards the sea by relatively steep slopes. This volcanic morphology is dissected by some deeply incised fluvial basins (i.e. Ribeira das Patas, in the S slope and Ribeiras do Paul, da Torre, Grande, de Alto Mira, da Garça and da Cruz on the N; Fig. 1c), while most other streams present a relatively

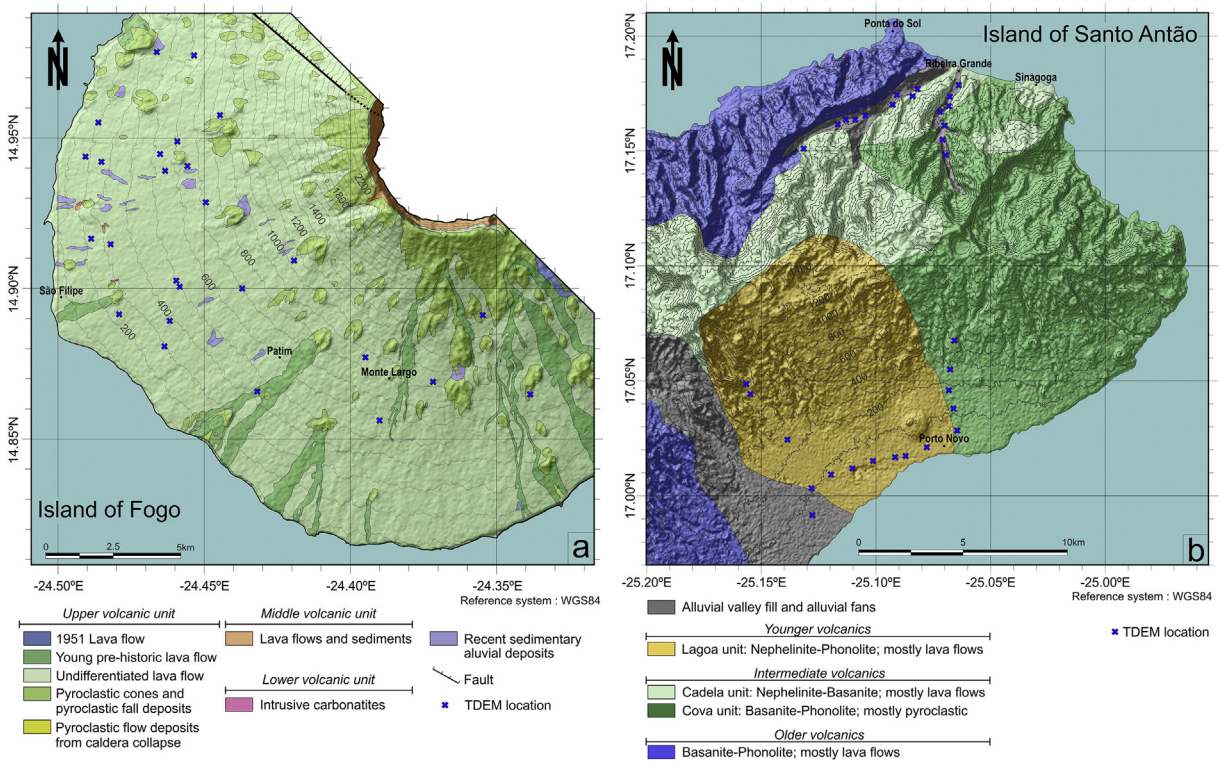

Fig. 2. Simplified geologic maps of the study areas in Fogo (b) and Santo Antão (c). The blue crosses indicate the TDEM soundings location. Geological sketch of Santo Antão modified from Holm et al. (2006). (For interpretation of the references to colour in this figure legend, the reader is referred to the web version of this article.)

incipient degree of incision. There is a marked contrast of the fluvial incision between the deeply carved N and S flanks as a result of the dominant NE-blowing trade winds. After crossing the ridge of the island, the wind is almost devoid of humidity so the rain is scarce and the landscape is arid in the S flank. The shore line presents the same contrast with taller cliffs due to the stronger wave erosion on the N coast when compared to the leeward littoral.

3. Method and survey setting

Time Domain Electromagnetic is based on the induction of a current waveform through a cable forming a loop on the surface followed by rapid current shut-offs. After each current shut-off, the disturbance through the transmitter loop generates a primary magnetic field that is in phase with the transmitter current. Later, a secondary magnetic field is created and its decay is measured by the receiver coil (Nabighian, 1988; Ward et al., 1990; Everett, 2013).

The apparent resistivity (ρ_a) is calculated through the mutual impedance Z(t) at time (t) as (see, e.g. Bortolozo et al., 2015):

$$\rho_a(t) = \left[\frac{\sqrt{\pi}a^2\, nb^2}{20Z\,(t)}\right]^{\frac{2}{3}} \left(\frac{\mu_0}{t}\right)^{\frac{5}{3}} \quad (1)$$

where a is the current loop radius and b the receiver loop radius, n represents the number of turns, and μ_0 the free space magnetic permeability. The apparent resistivity values for each sounding were inverted using an iterative approach based on the Levenberg-Marquardt method and Singular Value Decomposition (SVD) technique. This procedure can be seen as an optimization one where an initial model is modified until an expected misfit between data and model response is reached. The modification of the model (Δm) at iteration k is calculated by,

$$\left(\mathrm{J}\left(\mathrm{m}^k\right)^T \mathrm{J}\left(\mathrm{m}^k\right) + \lambda I\right)\Delta\mathrm{m} = -\mathrm{J}\left(\mathrm{m}^k\right)^T \mathrm{F}\left(\mathrm{m}^k\right) \quad (2)$$

where J is the Jacobian matrix, F represents the difference between data and model response in the logarithmic domain, λ is the damping factor and I the identity matrix. The system of equation is solved using the SVD technique.

The TDEM method was applied to detect the water-table depth and geometry in Fogo and Santo Antão islands. The high resistivity contrast between dry host rock and the saturated level allows determining the water-table depth below each measurement station. TDEM data was measured using the TEM-Fast48 equipment from Applied Electromagnetic Research (AEMR Inc.; Fainberg, 1999). This technique can be used in different configurations depending on the objectives to be achieved (Nicaise et al., 2013). The measurements were acquired in a single square loop configuration combining transmitter and receiver functions, with 50 × 50 m or 100 × 100 m loops depending on the terrain features. The data was processed with TEM-RES v.7.0 software from AEMR, which allows 1D modelling and inversion of the TDEM data. When necessary, the noisy data was firstly removed. The theoretical curve was fitted to the observed data applying trial-error methods and automatic inversion (Fig. 3). The fitting between modelled curves (lines in Fig. 3a, c) and data (points in the same fig.) was evaluated by direct observation since the program does not provide a quantitative assessment. The criterion in the selection of the final model is based on the minimum number of layers for the same quality of fitting.

In both islands the distribution of TDEM soundings is heterogeneous because of the rough topography and limited road access. In Fogo 26 soundings were performed on the southwest flank of the island covering an area of around 270 km^2 (Figs. 1b, 2a). The stations are as homogeneously distributed in the study area as possible, with spacing varying from 400 to 3500 m. In most soundings the loop dimension was 100 × 100 m with the applied current of 1 A (ampere). The soundings allowed depths of investigation of ~250 m on average providing a geoelectrical signature of the upper aquifer. A 3D view was obtained after 1D inversion of the data producing layers at each 50 m in depth, from 50 to 250 m below the surface. These layers where obtained extracting the resistivity values at each depth from the 1D inversion results and applying the kriging method with linear interpolation.

In Santo Antão 32 TDEM soundings were measured along 5 profiles on the north-eastern half of the island (Fig. 1c, 2b). The profiles on the northern slope were obtained along the valley bottoms of Ribeira Grande (P1) and Ribeira da Torre (P2) rivers. The remaining three profiles, on the southern flank of the island, followed the main roads of the area. Most soundings were performed using loops of 50 × 50 m with a transmitted current of 4 A. The investigation depth exceeded 100 m which allowed detecting the upper surface of the aquifers or deeper. 2D resistivity sections were created along the profiles using the sections mode of the TEM-RES program.

4. TDEM results

4.1. Island of Fogo

Most TDEM soundings were located at elevations between 250 and 750 m a.s.l. with the exception of 5 of them that are located higher and at maximum elevations of 1250 m a.s.l. (Fig. 2). No transient soundings were performed on coastal areas or inside the volcanically active caldera where most of the historical eruptions occurred.

The 3D view of the final models (Fig. 4) – composed of slices separated by 50 m in depth – shows that the 2 uppermost layers (at 50 and 100 m depths) detect high resistivities in excess of 1000 Ω·m (ohms × metre) in the higher elevations and resistivities between 500 and 1000 Ω·m in the lower topographic areas. There is a small area in the SW side of the island, near the coast line, that presents resistivities of about 200 Ω·m.

At the depth of 150 m lower resistivity values of ~15 Ω·m were obtained in a region located on the WSW side of the island, which extends towards the S. This southward extension of the very low resistivities is more evident at the depth of 200 m, while at this depth the resistivity for the higher elevation areas decreases below 1000 Ω·m. Finally, at 250 m depth most areas between 250 and 1000 m a.s.l. present resistivity values below 10 Ω·m.

It is important to mention that the coastal areas located on the SW side – mainly in the layer of 150 m depth – present resistivities lower than the adjacent ones due to the absence of TDEM sounding and to kriging interpolation effects (see marked area in Fig. 4). Thus, the model must be interpreted with caution in this area.

4.2. Santo Antão Island

Five profiles were inverted on the N (along the valleys of Ribeira Grande — P1 and Ribeira da Torre — P2) and S (along the main roads — P3 to P5) flanks of northeast Santo Antão (Fig. 5). The northern profiles have NW-SE (P1) and NNW-SSE (P2) orientations. All the TDEM soundings located at the N are located along the bottom of river valleys at low elevations (from 40 to 170 m a.s.l). Profile 1 is 7 km long and displays 3 layers separated by marked contrast in resistivity values. The shallower layer, with resistivities ranging from ~50 to ~100 Ω·m, has an average thickness of 50 m at higher elevations and ~20 m at lower altitudes. Below this layer the resistivity decreases to 5–10 Ω·m; this second layer has an average thickness of 60 m. The deepest layer presents even lower resistivity values of 1–5 Ω·m. The 4 km long profile 2, displays similar structure with the same resistivities and thicknesses.

The southern profiles have N-S (P3), WSW-ENE (P4) and NNW-SSE (P5) orientations and present much higher resistivities than the northern profiles. In P3 two layers can be differentiated: the shallower one has resistivity values higher than 1000 Ω·m and an average thickness of 100 m; the deeper layer presents intermediate resistivities ranging from 10 to 100 Ω·m. The resistivity pseudo-section produced by the

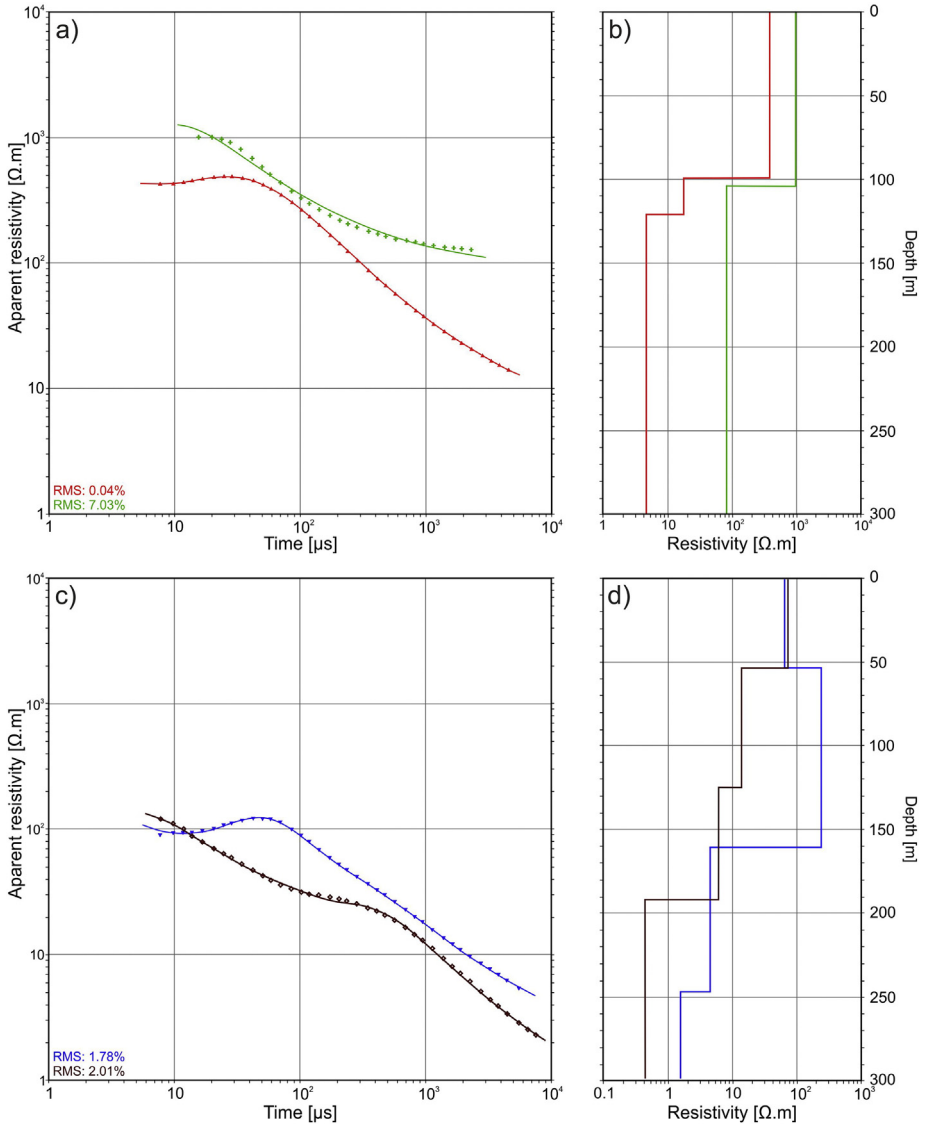

Fig. 3. TDEM curves and fitting (left) and models (right) of data from the Island of Fogo (a, b) and the Island of Santo Antão (c, d). The location of the four stations is shown in Fig. 1.

program – always done in horizontal layers – is not realistic due to the strong topographic contrast along the profile, and thus any interpretation should be made using the values displayed beneath the soundings locations.

In P4 three layers can be distinguished, in which the 2 shallowest are similar to those in profile 3 although presenting different thicknesses — about 40 m for the shallower and 60 m for the intermediate layer. The deepest layer presents low resistivity values of ~5 Ω·m, especially at the E extremity. Finally, P5 presents the same 2 upper layers but the resistivity contrast between them are smaller than in the previous profiles.

5. Discussion

5.1. Hydrogeology of Fogo

There are previous studies about groundwater resources in several islands of the Cape Verde archipelago, including the N flank of Fogo Island (Heilweil et al., 2006). Several geophysical methods have been applied on the island for water-table depth prospection; these include vertical electrical soundings (VES) and electromagnetic resistivity profiling (VLF-r) along the outer flanks of the island (Kallrén and Schreiber, 1988), and TDEM surveys within the central caldera (Descloitres et al., 2000). These investigations did not obtain successful results.

The island drainage system presents a centrifugal radial pattern composed of hundreds of shallow incised and weekly hierarchized watersheds that extend from the caldera rim to the sea. The most developed watersheds are those draining the N flank of the island. The studied area covered in this research is ~270 km^2 on the SW side of the Island of Fogo – ranging in altitude from sea level to 2500 m a.s.l. – where 26 TDEM soundings were measured.

The previous studies in Fogo hypothesize about groundwater distribution without the aid of good quality geophysical data. These studies claim that the water-table is at a relatively deep beneath the caldera (Kallrén and Schreiber, 1988; Barmen et al., 1990; Heilweil et al., 2009). The main conclusions obtained previously to our research are summarized as follows (Heilweil et al., 2012):

- water-table is approximately at sea level as measured in five wells located at altitudes of 20–60 m a.s.l.;
- occurrence of abundant coastal springs (Kallrén and Schreiber, 1988; Heilweil et al., 2006);
- water-table is present at 100 m and 180 m depths as determined from water drills located at altitudes of 300 m and 500 m a.s.l., respectively (Barmen et al., 1990);

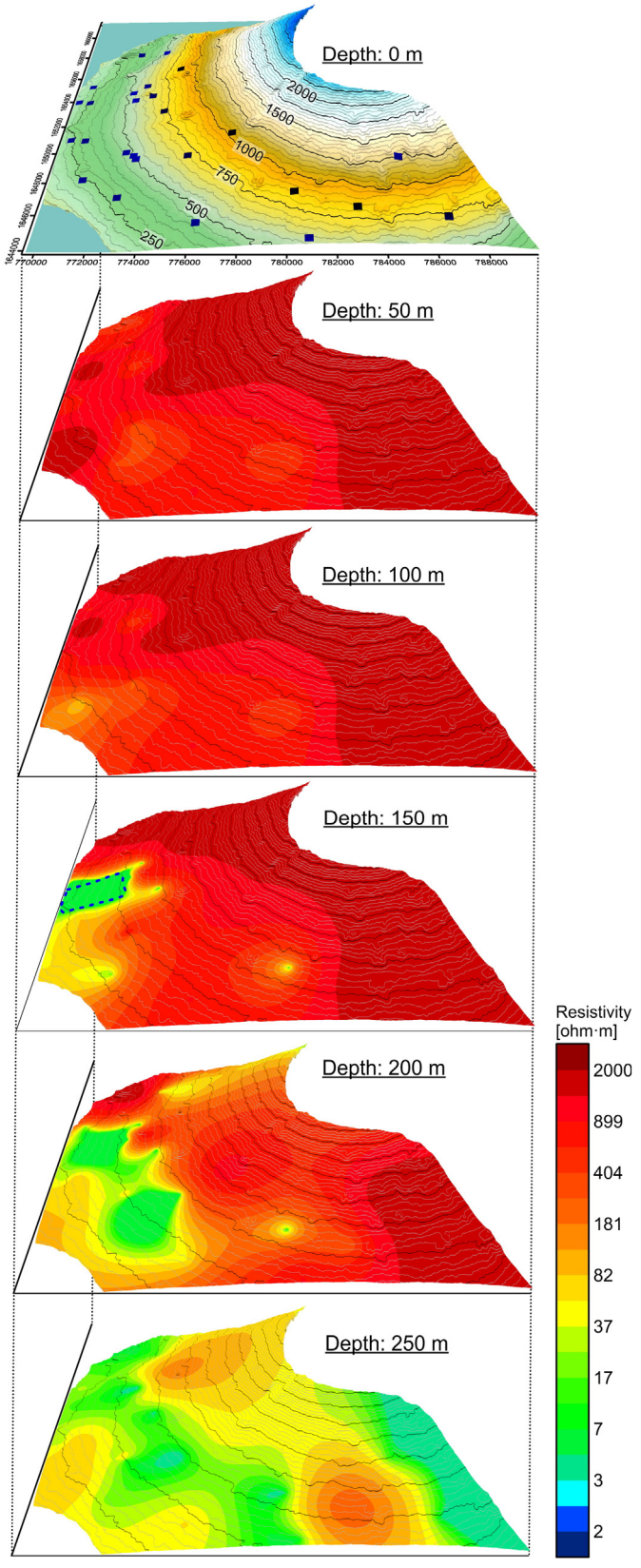

Fig. 4. 3D model of the subsurface resistivity distribution in southwest Fogo. The layers display the resistivity at every 50 m depth down to 250 m. The blue dots on the surface topographic map show the location of the TDEM stations. The blue dashed line indicates the area to be interpreted with caution due to kriging effects. (For interpretation of the references to colour in this figure legend, the reader is referred to the web version of this article.)

– water-table is deeper than 400 m beneath the caldera floor (Chã das Caldeiras) as determined from a geothermal research drill (Instituto Nacional de Gestão dos Recursos Hídricos, INGRH, 2011; http://www.ingrh.cv);
– TDEM surveys in Chã das Caldeiras found no evidence for the presence of water shallower than 400 m depth (Descloitres et al., 2000).

Our TDEM results indicate variable water-table depths depending on elevation (Fig. 6). High resistivities are obtained for the first 100 m below the topographical surface indicating that no water is present. Low resistivity values, indicating the presence of the water-table, appear for the first time at a depth of 150 m at elevations around 500 m a.s.l. on the west side of the study area (Fig. 4). This corresponds to the area between Monte Almada and the littoral spring of Praia Ladrão (Fig. 1b). The area with low resistivity presents a very geometrical (rectangular) shape suggesting a marked structural control – probably due to the presence of dikes – and possibly by the presence of a shallower old basement that crops out locally at Monte Almada. Low resistivities have been detected inland (up to around 750 m a.s.l.) at two soundings and to the SE at the depth of 200 m. Finally, at 250 m depth the low resistivity values extend to the whole study area up to 1000 m a.s.l. (Fig. 4). Therefore, at low topographic levels (up to 500 m a.s.l.) the water-table is located between 100 and 150 m depths, whereas in higher regions (up to 1000 m a.s.l.) the water-table is located at ~250 m depth. If we extrapolate this tendency to the island seaboard the water-table may be located at depths shallower than 100 m, while closer to the caldera rim it should be quite deep. These results are in general accordance with those obtained by Heilweil et al. (2012).

5.2. Hydrogeology of Santo Antão

Unlike the Island of Fogo, in Santo Antão there are no previous geophysical studies for water prospection, and just a few previous hydrology researches related to groundwater (Haagsma, 1995; Langworthy and Finan, 1997). For this study we measured 5 TDEM profiles corresponding to a total of 32 soundings. They cover the NE side of the island, with two profiles (P1 and P2) on the N flank and three profiles (P3–P5) in the S flank.

Remarkable differences in the resistivity values were found between the two flanks (Fig. 5). In the N profiles the average resistivity values for the unsaturated area is ~100 Ω·m, while in the S profiles resistivities are higher than 1000 Ω·m. Thus, there is a strong resistivity contrast with the northern profiles presenting resistivity values associated to the unsaturated area 10 times lower than the southern ones. Moreover, in the southern profiles P3 to P5 the water-table is deeper (~100 m) than in P1–P2 (~50–70 m).

In addition, the analysis of orthophoto image (Fig. 1c) shows marked humidity differences between the two flanks separated by the central mountain range that acts as the main water-divide of the island. These humidity differences can be highlighted comparing the dark brown shades for the N flank in contrast to the light brown ones representing the S flank; this is also expressed by the denser and more incised drainage of the slopes to the N of the central mountain range.

These contrasts in the humidity N-S conditions are explained by the action of the trade wind affecting the Cape Verde Islands (Chiapello et al., 1995). The condensation of the humidity transported by these winds, which blow almost continuously from the NE, corresponds to 1.5 to 3 times the amount of rainfall. The water vapour transported by the trade winds is condensed as the air masses climb the topographical barrier and are captured by the forest (Santamarta and Seijas, 2010). Therefore, the NE flank of the island receives most of the precipitation and the air masses that transpose the mountain range arrive to the S flank almost totally dry.

Furthermore, the northern profiles 1 and 2 (Fig. 5) show very low resistivity values, of ~1 Ω·m or lower on average, at depths of 130–100 m

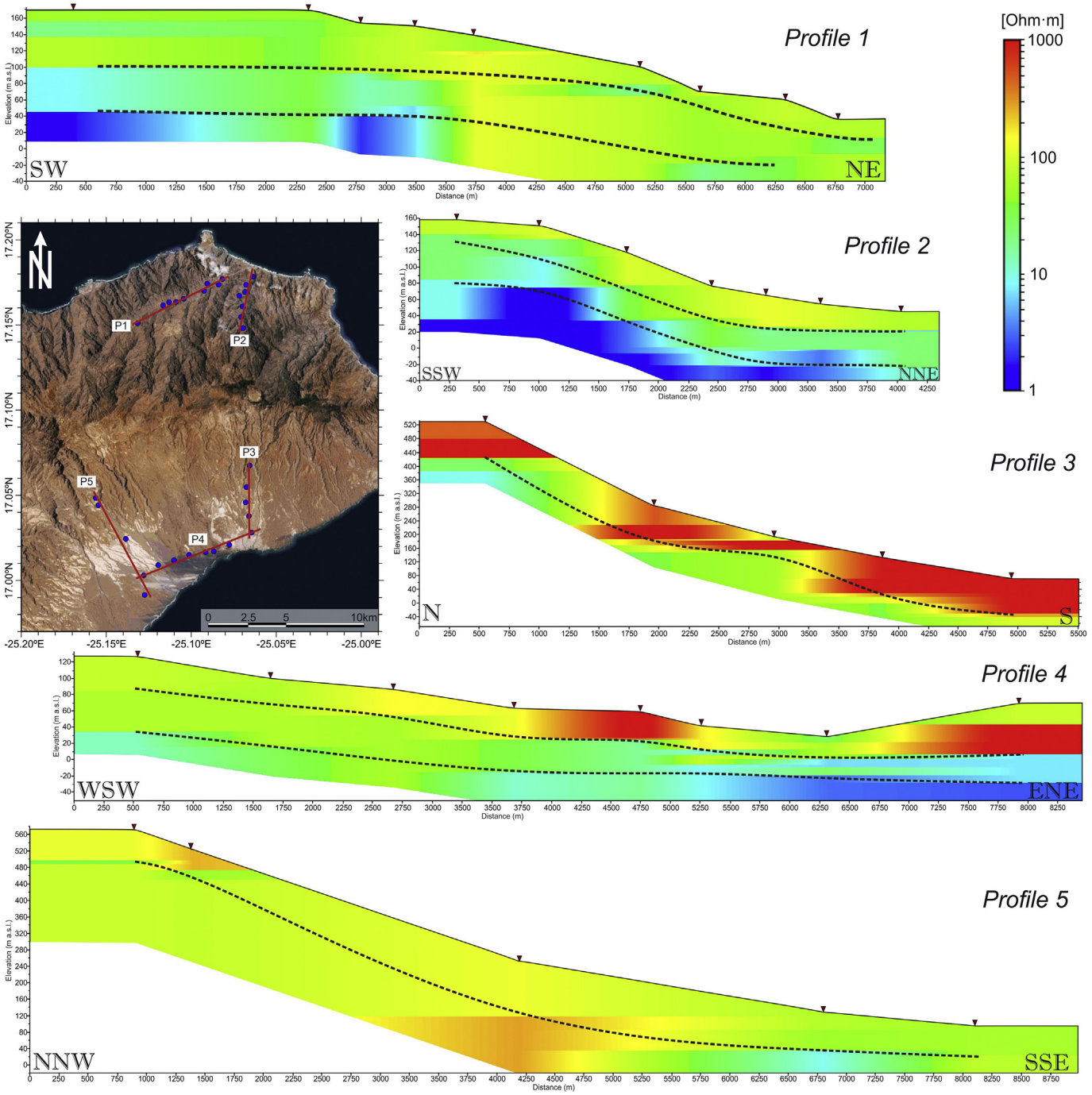

Fig. 5. Resistivity profiles and respective location in northeast Santo Antão. The blue dots on the orthophoto show the location of the TDEM stations and the red lines identify profiles P1 to P5. The dashed top lines indicate the water-table location and the bottom ones mark the fresh water-saltwater interface. (For interpretation of the references to colour in this figure legend, the reader is referred to the web version of this article.)

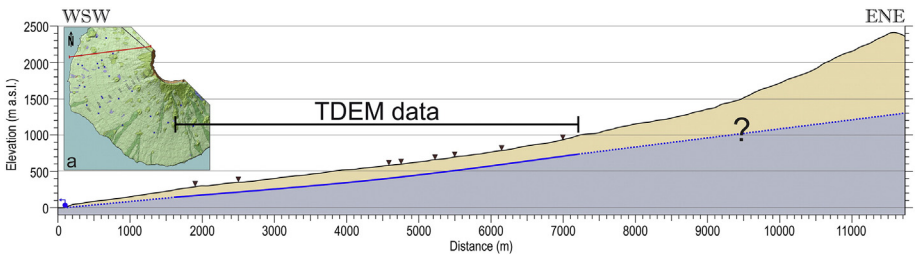

Fig. 6. Interpretative model of the water-table surface in southwest Fogo. The profile location is marked with a red line on the geological map. (For interpretation of the references to colour in this figure legend, the reader is referred to the web version of this article.)

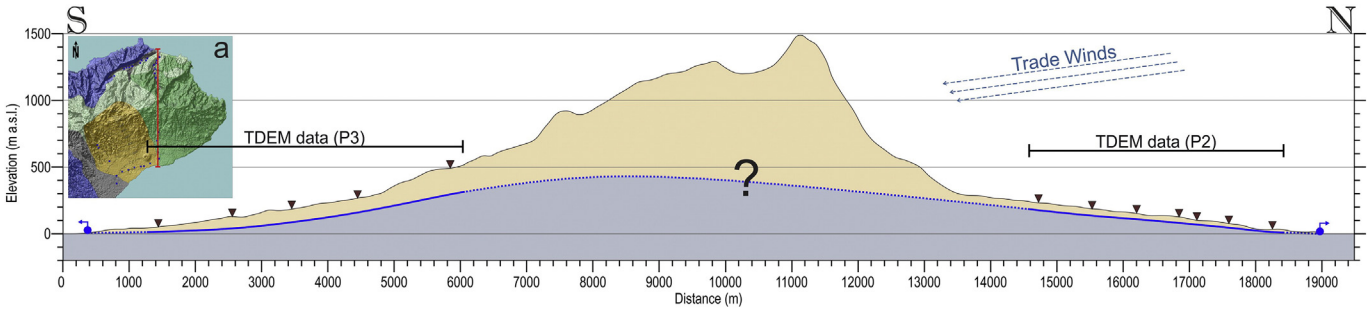

Fig. 7. Interpretative model of the water-table surface in northeast Santo Antão. The profile location is marked with a red line on the geological map. (For interpretation of the references to colour in this figure legend, the reader is referred to the web version of this article.)

indicating salt water intrusion. These intrusions reach altitudes of 40 m a.s.l. in P1 and around 80 m a.s.l. in P2 at the extremities further away from the shore line. This must be related with the fact that the valley bottoms of Ribeira Grande and Ribeira da Torre present a thick and highly permeable alluvial infill, with the volcanic basement below sea-level in the terminal part of their profile. This information was obtained from the owners of wells in the terminal few km of Ribeira Grande, which mentioned that the wells crossed thicknesses of gravel and sand exceeding the elevation of the site. Thus, the salt water intrusions in these areas must be taken into account when managing groundwater exploitation.

TDEM data obtained in both flanks of the island were used to obtain a hydrogeologic model of the water-table distribution in Santo Antão (Fig. 7). For this purpose, the data obtained in profiles 2 (N) and 3 (S) were used (Fig. 5). This model shows the differences in water-table depth in the two flanks; in the southern slope the water-table is deeper (~100 m depth) than in the northern slope (~50 m depth) due to the large differences in precipitation supplied by the trade winds. In addition, we interpolated the expected water-table morphology for the central part of the island, beneath the higher ranges of the volcanic edifice, which must be located at depths in excess of 1000 m.

The models of Figs. 6 and 7 must be taken as approximations to the water-table morphology, since our data does not allow depicting the effects of dikes swarms in the geometry of the main aquifer (Barmen et al., 1990). TDEM data allows obtaining a general model but the details of the aquifer compartments must be addressed in combination with additional geological and geophysical methods.

6. Conclusions

This study used TDEM data to provide new information on groundwater distribution in the islands of Fogo and Santo Antão (Cape Verde archipelago) where previous geophysical data was scarce. In Fogo a rough 3D resistivity distribution was obtained. It consists of a distribution of resistivity values covering the SW region of the island represented by successive layers below the surface at 50 m depth intervals, down to a depth of 250 m. The presence of a water-table was detected at a depth of 150 m close to the western coastal areas (up to elevations of 250 m a.s.l.), and at depths of 200–250 m for the whole study area up to altitudes of 1000 m a.s.l. The geometry of the water-table surface shows a shallower depth in littoral areas gradually increasing in depth up the slope.

TDEM data for Santo Antão was acquired along profiles located on the northern and southern slopes of the NE half of the island; the distribution was chosen in order to reflect the marked climatic differences between the wetter northern flank that directly receives the NE blowing dominant trade winds and the dryer southern flank. These differences are expressed in the resistivity values obtained by the TDEM profiles. In the N slope the water-table is shallower than in the S. Additionally the data allowed detecting important salt water intrusion in the N flank profiles, as well as estimating the expected geometry of the main aquifer surface across the island, interpreted to be located at greater depths beneath the higher reaches of the volcanic edifice.

This study demonstrates the usefulness of TDEM methods for groundwater prospection, using both profile and areal station geometries. Our results provided an approximate initial groundwater model distribution in the islands of Fogo and Santo Antão in the Republic of Cape Verde. However this is only an approximation that must be complemented with more detailed geological and geophysical studies.

Acknowledgements

The authors thank GESTO Energy Consulting for permission to use the data. In addition, we are grateful with the positive comments and suggestions made by two anonymous reviewers. This publication is supported by project FCT UID/GEO/50019/2013 — Instituto Dom Luiz.

References

Ancochea, E., Huertas, M.J., Hernán, F., Brändle, J.L., 2010. Volcanic evolution of São Vicente, Cape Verde Islands: the Praia Grande landslide. J. Volcanol. Geotherm. Res. 198, 143–157.

Ancochea, E., Huertas, M.J., Hernán, F., Brändle, J.L., 2014. A new felsic cone-sheet swarm in the Central Atlantic Islands: the cone-sheet swarm of Boa Vista (Cape Verde). J. Volcanol. Geotherm. Res. 274, 1–15.

Ancochea, E., Huertas, M.J., Hernán, F., Brändle, J.L., Alonso, M., 2015. Structure, composition and age of the small islands of Santa Luzia, Branco and Raso (Cape Verde Archipelago). J. Volcanol. Geotherm. Res. 302, 257–272.

Barmen, G., Carvalho, V., Querido, A., 1990. Groundwater-related geological and isotopic investigations on the Island of Fogo: an overview. Report LUTVDG/TVTG-90/3027. Lund University Institute of Technology, Lund, Sweden (72 pp.

Bortolozo, C.A., Porsani, J.L., Santos, F.A.M.d., Almeida, E.R., 2015. VES/TEM 1D joint inversion by using Controlled Random Search (CRS) algorithm. J. Appl. Geophys. 112, 157–174.

Brum da Silveira, A., Madeira, J., Serralheiro, A., 1997. A estrutura da ilha do Fogo, Cabo Verde. A erupção vulcânica de 1995 na ilha do Fogo, Cabo Verde. Instituto de Investigação Científica Tropical e Ministério da Ciência e Tecnologia, pp. 63–78.

Chiapello, I., Bergametti, G., Gomes, L., Chatenet, B., Dulac, F., Pimenta, J., Santos Suares, E., 1995. An additional low layer transport of Sahelian and Saharan dust over the north-eastern tropical Atlantic. Geophys. Res. Lett. 22, 3191–3194.

Custodio, E., 1978. Geohidrología de terrenos e islas volcánicas. Centro de estudios Hidrográficos, Madrid.

Day, S.J., Heleno da Silva, S.I.N., Fonseca, J.F.B.D., 1999. A past giant lateral collapse and present-day flank instability of Fogo, Cape Verde Islands. J. Volcanol. Geotherm. Res. 94, 191–218.

Descloitres, M., Guérin, R., Albouy, Y., Tabbagh, A., Ritz, M., 2000. Improvement in TDEM sounding interpretation in presence of induced polarization. A case study in resistive rocks of the Fogo volcano, Cape Verde Islands. J. Appl. Geophys. 45, 1–18.

Descloitres, M., Chalikakis, K., Legchenko, A., Moussa, A.M., Genthon, P., Favreau, G., Le Coz, M., Boucher, M., Oï, M., 2013. Investigation of groundwater resources in the Komadugu Yobe Valley (Lake Chad Basin, Niger) using MRS and TDEM methods. J. Afr. Earth Sci. 87, 71–85.

Duprat, H.I., Friis, J., Holm, P.M., Grandvuinet, T., Sørensen, R.V., 2007. The volcanic and geochemical development of São Nicolau, Cape Verde Islands: constraints from field and $^{40}Ar/^{39}Ar$ evidence. J. Volcanol. Geotherm. Res. 162, 1–19.

Dyhr, C.T., Holm, P.M., 2010. A volcanological and geochemical investigation of Boa Vista, Cape Verde Islands; $^{40}Ar/^{39}Ar$ geochronology and field constraints. J. Volcanol. Geotherm. Res. 189, 19–32.

Eisele, S., Freundt, A., Kutterolf, S., Ramalho, R.S., Kwasnitschka, T., Wang, K.L., Hemming, S.R., 2015. Stratigraphy of the Pleistocene, phonolitic Cão Grande Formation on Santo Antão, Cape Verde. J. Volcanol. Geotherm. Res. 301, 204–220.

Everett, M.E., 2013. Near-surface Applied Geophysics. Cambridge University Press, UK 415 pp.
Fainberg, E., 1999. TEM-Fast 48 Manual. Applied Electromagnetic Research, Amsterdam, The Netherlands.
Figueira, C., de Sequeira, M.M., Vasconcelos, R., Prada, S., 2013. Cloud water interception in the temperate laurel forest of Madeira Island. Hydrol. Sci. J. 58, 152–161.
Flint, A.L., Flint, L.E., Hevesi, J.A., Blainey, J.B., 2013. Fundamental concepts of recharge in the desert southwest: a regional modeling perspective. In: Hogan, J.F., Phillips, F.M., Scanlon, B.R. (Eds.), Groundwater Recharge in a Desert Environment: The Southwestern United States. American Geophysical Union, pp. 159–184.
Gingerich, S.B., Oki, D.S., 2000. Ground Water in Hawaii. U.S. Geological Survey, Fact Sheet 126-00 6 pp.
Goldman, M., Rabinovich, B., Rabinovich, M., Gilad, D., Gev, I., Schirov, M., 1994. Geophysics and environment application of the integrated NMR-TDEM method in groundwater exploration in Israel. J. Appl. Geophys. 31, 27–52.
Haagsma, B., 1995. Traditional water management and state intervention: the case of Santo Antão, Cape Verde. Mt. Res. Dev. 15, 39–56.
Healy, R.W., 2010. Estimating groundwater recharge. Cambridge University Press, Cambridge, UK.
Heilweil, V.M., Earle, J.D., Cederberg, J.R., Messer, M.M., Jorgensen, B.E., Verstraeten, I.M., Moura, M.A., Querido, A., Spencer, S., Osorio, T., 2006. Evaluation of Baseline Ground-water Conditions in the Mosteiros, Ribeira Paul, and Ribeira Fajã Basins, Republic of Cape Verde, West Africa, 2005–06. US Department of the Interior, US Geological Survey.
Heilweil, V.M., Solomon, D.K., Gingerich, S.B., Verstraeten, I.M., 2009. Oxygen, hydrogen, and helium isotopes for investigating groundwater systems of the Cape Verde Islands, West Africa. Hydrogeol. J. 17, 1157–1174.
Heilweil, V.M., Healy, R.W., Harris, R.N., 2012. Noble gases and coupled heat/fluid flow modeling for evaluating hydrogeologic conditions of volcanic island aquifers. J. Hydrol. 464–465, 309–327.
Hoareau, J., Vouillamoz, J.M., Beck, M., Reddy, M., Descloitres, M., Legchenko, A., Sekhar, M., Kumar, M.M., Braun, J.-J., 2007. Joint use of geophysical and hydrological methods to characterize structures and flow geometry in a complex aquifer. Near Surface 2007—13th EAGE European Meeting of Environmental and Engineering Geophysics.
Hoernle, K., Tilton, G., Le Bas, M.J., Duggen, S., Garbe-Schönberg, D., 2002. Geochemistry of oceanic carbonatites compared with continental carbonatites: mantle recycling of oceanic crustal carbonate. Contrib. Mineral. Petrol. 142, 520–542.
Holm, P.M., Wilson, J.R., Christensen, B.P., Hansen, L., Hansen, S.L., Hein, K.M., Mortensen, A.K., Pedersen, R., Plesner, S., Runge, M.K., 2006. Sampling the Cape Verde mantle plume: evolution of melt compositions on Santo Antão, Cape Verde Islands. J. Petrol. 47, 145–189.
Holm, P.M., Grandvuinet, T., Friis, J., Wilson, J.R., Barker, A.K., Plesner, S., 2008. An ^{40}Ar–^{39}Ar study of the Cape Verde hot spot: temporal evolution in a semistationary plate environment. J. Geophys. Res. Solid Earth 113.
Instituto Nacional de Gestão dos Recursos Hídricos, INGRH (Ed.), 2011. Relatorio de actividade do INGRH. Cape Verde.
Jackson, D.B., Lenat, J.F., 1989. High-level Water Tables on Hawaiian Type Volcanoes and Intermediate Depth Geoelectric Structures, Kilauea Volcano, Hawaii and Piton de la Fournaise Volcano, Isle de la Reunion. New Mexico Bureau of Geology & Mineral Resources, pp. 131–142.
Johnson, M.E., Ramalho, R.S., Baarli, B.G., Cachão, M., da Silva, C.M., Mayoral, E.J., Santos, A., 2014. Miocene–Pliocene rocky shores on São Nicolau (Cape Verde Islands): contrasting windward and leeward biofacies on a volcanically active oceanic island. Palaeogeogr. Palaeoclimatol. Palaeoecol. 395, 131–143.
Kallrén, L., Schreiber, I., 1988. Groundwater survey on western Fogo, Cape Verde. Report TVTG-5019. Lund Institute of Technology, Lund, Sweden.
Langworthy, M., Finan, T.J., 1997. Waiting for Rain: Agriculture and Ecological Imbalance in Cape Verde. Lynne Rienner Publishers.
Liu, C.C., Lau, L.S., Mink, J.F., 1983. Ground water model for a thick fresh water lens. Ground Water 21, 293–300.
López-Guzmán, T., Alector Ribeiro, M., Orgaz-Agüera, F., Marmolejo Martín, J.A., 2015. El turismo en Cabo Verde: Perfil y valoración del viajero. Estud. Perspect. Tur. 24, 512–528.
Macdonald, G.A., Abbott, A.T., Peterson, F.L., 1983. Volcanoes in the Sea: The Geology of Hawaii. 2nd edn. University of Hawaii Press, Honolulu.
Madeira, J., Brum da Silveira, A., Mata, J., Mourão, C., Martins, S., 2008. The role of mass movements on the geomorphologic evolution of island volcanoes: examples from Fogo and Brava in the Cape Verde archipelago. Comun. Geol. 95, 93–106.
Madeira, J., Mata, J., Mourão, C., da Silveira, A.B., Martins, S., Ramalho, R., Hoffmann, D.L., 2010. Volcano-stratigraphic and structural evolution of Brava Island (Cape Verde) based on $^{40}Ar/^{39}Ar$, U–Th and field constraints. J. Volcanol. Geotherm. Res. 196, 219–235.
Marques, R., Prudêncio, M.I., Waerenborgh, J.C., Rocha, F., Dias, M.I., Ruiz, F., Ferreira da Silva, E., Abad, M., Muñoz, A.M., 2014. Origin of reddening in a paleosol buried by lava flows in Fogo island (Cape Verde). J. Afr. Earth Sci. 96, 60–70.
Martí, J., Hurlimann, M., Ablay, G.J., Gudmundsson, A., 1997. Vertical and lateral collapses on Tenerife (Canary Islands) and other volcanic ocean islands. Geology 25, 879–882.
Mitchell, J.G., Le Bas, M.J., Zielonka, J., Furnes, H., 1983. On dating the magmatism of Maio, Cape Verde Islands. Earth Planet. Sci. Lett. 64, 61–76.
Nabighian, M.N., 1988. Electromagnetic Methods in Applied Geophysics. SEG Books.
Nicaise, Y., Marc, D., Michel, V.J., Christian, A., 2013. Delimitation of the salt water wedge in the shallow coastal aquifer by TDEM method at Togbin (South Benin). Int. J. Adv. Sci. Technol.
Plesner, S., Holm, P.M., Wilson, J.R., 2003. ^{40}Ar–^{39}Ar geochronology of Santo Antão, Cape Verde Islands. J. Volcanol. Geotherm. Res. 120, 103–121.
Ramalho, R., Helffrich, G., Schmidt, D., Vance, D., 2010. Tracers of uplift and subsidence in the Cape Verde archipelago. J. Geol. Soc. 167, 519–538.
Ramalho, R.S., Winckler, G., Madeira, J., Helffrich, G.R., Hipólito, A., Quartau, R., Adena, K., Schaefer, J.M., 2015. Hazard potential of volcanic flank collapses raised by new megatsunami evidence. Sci. Adv. 1, e1500456.
Ribeiro, O., 1960. A Ilha do Fogo e as suas Erupções-Memórias. (Série geográfica I), Junta de Investigação do Ultramar. 2nd Ed. Lisboa, Portugal. 319 pp. In Portuguese, Lisboa (Portugal).
Ruiz-Constán, A., Pedrera, A., Martos-Rosillo, S., Galindo-Zaldívar, J., Martín-Montañés, C., González De Aguilar, J.P., 2015. Structure of a complex carbonate aquifer by magnetic, gravity and TDEM prospecting in the JAÉN area, Southern Spain. Geol. Acta 13, 191–203.
Sananikone, K., 1998. Subsurface Characterization Using Time-domain Electromagnetics at the Texas a&M University Brazos River Hydrologic Field Site, Burleson County, Texas. Texas A&M University.
Santamarta Cerezal, J.C., 2013. Hidrología y recursos hídricos en islas y terrenos volcánicos. Colegio de Ingenieros de Montes, Tenerife.
Santamarta Cerezal, J.C., Seijas Bayón, J., 2010. Fundamentos y tecnologías para la captación y uso del agua procedente de la lluvia horizontal en los montes canarios. Montes: revista de ámbito forestal 100, pp. 15–21.
Torres, P.C., Madeira, J., Silva, L.C., Brum da Silveira, A., Serralheiro, A., Mota Gomes, A., 1998. Carta geológica da Ilha do Fogo (República de Cabo Verde): erupçoes históricas e formaçoes enquadrantes. Geological Map. Ed. Lattex, 1 Sheet at 1:25.000 Scale.
Torres, P., Silva, L., Serralheiro, A., Tassinari, C., Munhá, J., 2002. Enquadramento geocronológico pelo método K/Ar das principais sequências vulcano-estratigráficas da Ilha do Sal—Cabo Verde. Garcia de Orta, Série Geológica 18, pp. 9–13.
Ward, S.H., Hoekstra, P., Blohm, M.W., 1990. 1. Case histories of time-domain electromagnetic soundings in environmental geophysics. Geotechnical and Environmental Geophysics. Society of Exploration Geophysicists, pp. 1–16.
White, R.S., 1989. Asthenospheric control on magmatism in the ocean basins. Geol. Soc. Lond., Spec. Publ. 42, 17–27.
Yechieli, Y., Kafri, U., Goldman, M., Voss, C., 2001. Factors controlling the configuration of the fresh–saline water interface in the Dead Sea coastal aquifers: synthesis of TDEM surveys and numerical groundwater modeling. Hydrogeol. J. 9, 367–377.